The interaction of ions with nonpolar neutrals: The collision broadening of ion cyclotron resonance lines of ions in hydrogen and methane

D. P. Ridge*

Department of Chemistry, University of Delaware, Newark, Delaware 19711 †
and Noyes Laboratory of Chemical Physics, California Institute of Technology, Pasadena, California 91109

J. L. Beauchamp‡

Noyes Laboratory of Chemical Physics, California Institute of Technology, Pasadena, California 91109
(Received 26 June 1974)

The motion of ions in an ion cyclotron resonance cell is considered, and measurements of ion cyclotron resonance linewidths are described. The connection between cyclotron resonance linewidths and kinetic parameters is developed. Mobilities and collision frequencies of CH_5^+, $C_2H_5^+$, $C_3H_7^+$, $C_4H_9^+$, and Na^+ in methane and H^+, H_3^+, H_3O^+, CH_5^+, $C_2H_5^+$, $C_3H_7^+$, and Na^+ in hydrogen are determined from the linewidth measurements. Resulting mobilities of H^+, H_3^+, and Na^+ in H_2 are found to agree well with drift tube measurements, in contrast to previous cyclotron resonance linewidth determinations. The mobilities are interpreted in terms of three model ion molecule interaction potentials. The mobilities are found to be in general consistent with both a three term 12–6–4 potential and an acentric potential but not with the simple polarization potential. Potential parameters consistent with binding energies from the literature and the present mobility measurements are reported for H_3^+–H_2, CH_5^+–CH_4, and $C_2H_5^+$–CH_4.

INTRODUCTION

Ion cyclotron resonance studies of ion–molecule reactions are normally accomplished in the pressure range between 10^{-7} and 10^{-5} torr.[1–3] In the usual experimental arrangement, the ions generated by electron impact are drifted through the cell by the action of crossed electric and magnetic fields (Fig. 1), with the drift velocity being given by

$$v_d = cE/H \ . \tag{1}$$

With the typical values $E = 0.5$ V/cm and $H = 7.5$ kG, the drift velocity is 6.7×10^3 cm/sec, corresponding to an ion transit time through the resonance region of $\tau = 10^{-3}$ sec. In an ion–molecule reaction, considerable conversion of reactant to product occurs when the quantity $nk\tau$ approaches unity, where n is the number density of the neutral species and k represents the bimolecular reaction rate constant.[4] Ion–molecule reaction rate constants are typically 10^{-9} cm^3 molecule^{-1} · sec^{-1}.[4] Consequently, $nk\tau$ approaches unity at a particle density of $\sim 3\times10^{-5}$ torr. Below this pressure, ion cyclotron resonance line shapes are not significantly collision broadened, since the ion suffers at most one collision as it passes through the cell. At higher pressures, appreciable collision broadening of the absorption peak occurs with a concomitant decrease in resolution. In the case of methane, these various factors are illustrated in Fig. 2. CH_5^+, evident at m/e 17 in Fig. 2, is produced in the well-known reaction

$$CH_4^+ + CH_4 \rightarrow CH_5^+ + CH_3 \tag{2}$$

which proceeds with a bimolecular rate constant $k = 1.1 \pm 0.1\times10^{-9}$ cm^3 molecule^{-1} · sec^{-1} at thermal ion energies.[1,4] The reactant has totally disappeared and the product ion peak is significantly broadened at 5.32×10^{-4} torr. At 1.80×10^{-3} torr, the line broadening has increased to the extent that resolution of adjacent mass peaks would be impeded.

While the loss of resolution limits the usefulness of ion cyclotron resonance spectroscopy for the study of ion–molecule reactions, an analysis of the collisional broadening phenomenon can provide important information about nonreactive collision processes. This is, in general, supported by the experimental results of Wobschall and co-workers,[5] by the present results,[6] by the results of Dymerski and Dunbar,[7] by Buttrill's results,[8] and by Huntress' results.[9]

The present study is an examination of the collision broadening of the cyclotron resonance absorptions of ions in methane and hydrogen. Both methane and hydrogen are extensively utilized as chemical ionization reagents in high pressure mass spectrometric studies. Minor constituents present in methane and hydrogen are ionized by reaction with CH_5^+ and $C_2H_5^+$ in methane and H_3^+ in hydrogen. Using chemical ionization reactions, it is possible to generate a wide variety of ionic species in methane and hydrogen for the study of collisional broadening processes. Such studies yield collision frequencies for momentum transfer, diffusion cross sections, and ion mobilities. These data are useful in providing a more complete description of ion motion in chemical ionization experiments, particularly in regard to the important questions of ion source residence time, collision frequencies, and the establishment of thermal equilibrium. The data are also essential to a proper understanding of the kinetics of ion–molecule reactions.

Ion mobilities for several of the systems studied have been measured using drift tube techniques. Comparison of drift tube and ion cyclotron resonance measurements provides a useful test of both techniques. McDaniels[10] and co-workers have reported the mobility of H_3^+ in hydrogen. They obtain a value of 11.1 ± 0.6 cm^2 V^{-1} · sec^{-1} in the limit of low E/P (ratio of electric field strength to pressure). Two measurements of the H_3^+ hydrogen mobility using ion cyclotron resonance techniques are

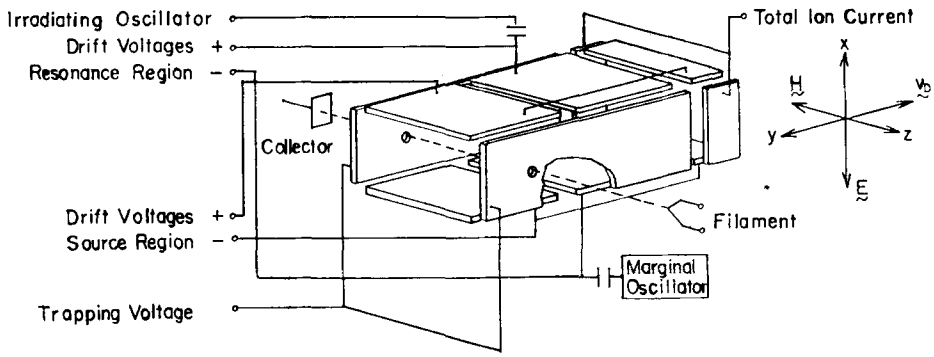

FIG. 1. Cutaway view of cyclotron resonance cell. The magnetic field is collinear with the electron beam.

not in agreement. Huntress[9] reported 10.9 ± 0.2 $cm^2 V^{-1} \cdot sec^{-1}$ in good agreement with the drift tube results, but Wobschall[5] reported 7.2 $cm^2 V^{-1} \cdot sec^{-1}$. Huntress measured the power absorption at resonance as a function of pressure, and Wobschall measured the width of the resonance as a function of pressure. To provide confidence in cyclotron resonance techniques for ion mobility measurements, it is essential that this discrepancy be resolved.

Patterson has measured the mobility of SF_5^- and SF_6^- in methane[11] at low E/P. The only other study of the mobilities of ions in methane which provided for mass identification of the charge carriers is that of Meisels and co-workers.[12] The apparatus used in that study was designed for chemical ionization studies, and only relative drift velocities could be determined with any accuracy. The present results are therefore a significant addition to data available on the motion of ions in methane.

As a transport property, ionic mobility can be treated by the kinetic theory of gases and information about the ion–molecule interaction potential obtained. The procedure is to assume an algebraic form of the potential in terms of unspecified parameters and calculate the mobility as a function of these parameters using the kinetic theory. The unspecified parameters are then determined by comparison of calculated and experimental mobilities. This is the procedure that has been used extensively to determine neutral–neutral interaction potentials from gas transport properties. The necessary calculations have been done for three algebraic potentials given in Eqs. (3)–(5),

$$V(r) = \infty \qquad r < D_{12}$$
$$V(r) = -\alpha q^2/2r^4 \quad r > D_{12}\,, \tag{3}$$

$$V(r) = \frac{\epsilon}{2}\left[(1+\gamma)\left(\frac{r_m}{r}\right)^{12} - 4\gamma\left(\frac{r_m}{r}\right)^{6} - 3(1-\gamma)\left(\frac{r_m}{r}\right)^{4}\right], \tag{4}$$

$$V(r) = \frac{\epsilon}{2}\left[\left(\frac{r_m - a}{r - a}\right)^{12} - 3\left(\frac{r_m - a}{r - a}\right)^{4}\right], \tag{5}$$

where r is the distance between the centers of mass of the ion and molecule, α is the angle averaged polarizability of the neutral, q is the electron charge, D_{12} is the hard sphere radius, ϵ and r_m are the depth and position of the potential minima, γ is a measure of the relative importance of the r^{-6} and r^{-4} terms in the 12–6–4 potential [Eq. (4)], and a is the acentric parameter of the acentric potential [Eq. (5)]. The Langevin potential [Eq. (3)] includes the long range ion–induced dipole interaction and treats ion and molecule structure in the simplest possible way: as hard spheres.[13] Mason and Schamp used a more realistic r^{-12} repulsive interaction and included an r^{-6} term to account for ion-induced quadrupole and dispersion forces. Using this potential, Mason and Schamp were able to account for the magnitudes and temperature variation of the mobilities of alkali metal ions in rare gases.[14] The acentric potential [Eq. (5)] was proposed to account for the constraints on the charge distributions of polyatomic species. It has proved useful in accounting for other transport properties of polyatomic species, and Mason and O'Hare have recently used it to calculate mobilities.[15]

The hard sphere potential has one disposable parameter, D_{12}. Although the 12–6–4 and acentric potentials appear to have three disposable parameters, one pa-

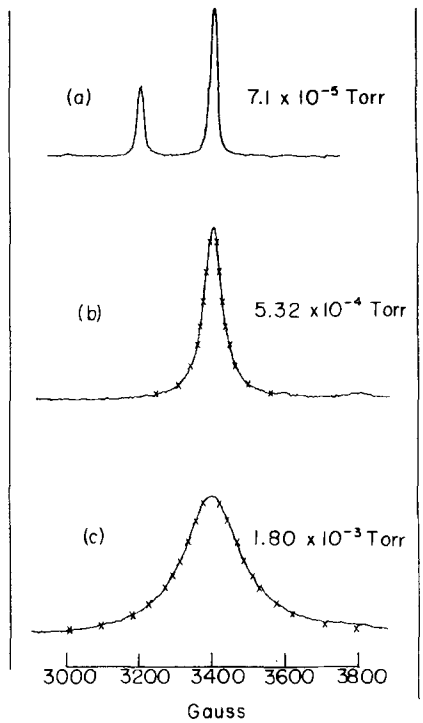

FIG. 2. Methane spectrum at 14 eV and various pressures. The resonances at 3200 and 3400 G correspond to CH_4^+ and CH_5^+, respectively. The points marked on the spectra indicate a fixed Lorentzian line.

rameter is fixed in each case by the requirement that the potential approach the ion–induced dipole potential asymptotically. This requirement gives

$$3\epsilon r_m^4(1-\gamma)=e^2\alpha\,, \tag{6}$$

$$3\epsilon(r_m-a)^4=e^2\alpha\,. \tag{7}$$

Since all three potentials have the same asymptotic behavior, they all give the same low temperature low field limit for the mobility. This limit, K_p, is given by

$$K_p=\frac{1}{n2.210\pi\mu^{1/2}\alpha^{1/2}}\,, \tag{8}$$

where μ is the reduced mass of the ion–neutral pair and n is the neutral number density. If the neutral number density is that of an ideal gas at 273.15 °K and 760 torr pressure (2.688×10^{19} molecules cm^{-3}), then K_p is denoted K_p^0 and is given in $cm^2V^{-1}\cdot sec^{-1}$ by

$$K_p^0=\frac{13.876}{\alpha^{1/2}\mu^{1/2}} \tag{9}$$

where α is in $Å^3$ and μ is in atomic mass units. The low field mobility calculated from each of the potentials is expressed in terms of K_p by

$$\frac{K}{K_p}=\frac{1.799(1-\gamma)^{1/2}}{(T^*)^{1/2}\Omega^{(1,1)*}(T^*,a^*)}\,, \tag{10}$$

$$\frac{K}{K_p}=\frac{1.799(1-a^*)^2}{(T^*)^{1/2}\Omega^{(1,1)*}(T^*,a^*)}\,, \tag{11}$$

$$\frac{K}{K_p}=\frac{A(\lambda)}{0.5105}\,, \tag{12}$$

where T^* is kT/ϵ and a^* is a/r_m. The collision integrals $\Omega^{(1,1)*}(T^*,\gamma)$ and $\Omega^{(1,1)*}(T^*,a^*)$ and $A(\lambda)$ are tabulated in the literature.[14–16] The notation $\Omega^{(1,1)*}(T^*,\gamma)$ indicates that $\Omega^{(1,1)*}$ is a function of T^* and γ. The parameter λ upon which $A(\lambda)$ depends is defined by

$$\lambda^2=\frac{2kT}{\alpha e^2}D_{12}^4\,. \tag{13}$$

The variation of K with λ^2 corresponds to the variation of K with temperature for a given ion–molecule pair or the variation of K with ion size for a series of ions in a particular gas at a fixed temperature. Parameters analogous to λ^2 for the 12–6–4 and acentric potentials are given by

$$\frac{T^*}{1-\gamma}=\frac{3kT}{\alpha e^2}r_m^4\,, \tag{14}$$

$$\frac{T^*}{(1-a^*)^4}=\frac{3kT}{\alpha e^2}r_m^4\,, \tag{15}$$

which follow directly from Eqs. (6) and (7), respectively. The left hand side expressions in Eqs. (14) and (15) are used as size parameters in discussing the present results. Equation (16),

$$\lambda^2=\frac{2}{3}\left(\frac{T^*}{1-\gamma}\right)\left(\frac{D_{12}}{r_m}\right)^4\,, \tag{16}$$

derived from Eqs. (13) and (14), is useful in comparing the Langevin theory with the more recent theories. The relationship between D_{12} and r_m is given by Patterson.[11]

EXPERIMENTAL

Ion cyclotron resonance spectra were recorded in the absorption mode by modulating the electron energy[17] and feeding the output of the marginal oscillator into a Princeton Applied Research Model HR-8 phase sensitive detector referenced to the modulation frequency (32 cps). Typical spectra are shown in Fig. 2. Linewidths measured from absorption spectra were compared with linewidths from derivative spectra obtained by field modulation. As required for a Lorentzian line shape, the spacing of the maximum and minimum of the derivative spectrum is given by $2\xi/\sqrt{3}$. This yielded collision frequencies identical to those measured from absorption linewidths. Electron energy modulation proved to be more sensitive in the present application because of the limited amplitude of field modulation which could be generated for detecting wide lines. All spectra were recorded by sweeping the magnetic field strength at constant observing frequency.

An MKS Instruments model 90H1E capacitance manometer was employed to determine pressure. The capacitance manometer was calibrated against a Bendix GM-100A McLeod gauge. Both gauges were connected to a test vacuum manifold. Helium gas was used to minimize mercury pumping error.[18] The gas was admitted to the system and the pressure read on both gauges. The McLeod gauge and the capacitance manometer agreed to within less than 1%. The capacitance manometer was operated at 65 °C to minimize zero drift, so it was necessary to correct the lower pressure readings for thermal transpiration.[19] Immediately following the calibration, the capacitance manometer was removed from the test stand and connected to the ion cyclotron resonance spectrometer and the collision frequency of CH_5^+ in CH_4 measured as described in the Results below. The gauge was allowed to cool to room temperature and equilibrate overnight. The next day the CH_5^+ collision frequency was measured again. The ratio of the two measured collision frequencies was 1.066, in good agreement with the theoretical thermal transpiration correction, $(338/297)=1.068$[19]. Na^+ ions were produced by heating a mineral containing the alkali metal. The mineral was prepared following the description of Blewett and Jones[20] and melted in a platinum crucible. A filament of 5 mil platinum wire was dipped into the melt so that a bead formed on the filament. The filament was mounted on the cell so that the bead went through a hole in the trapping plate in the source region of the cell (Fig. 1). The bead was heated by passing a current through the wire. All gases employed were obtained from Matheson and had a stated purity of greater than 99%. Gas mixtures were prepared manometrically, with freeze–pump–thaw cycles used to degas additives to methane and hydrogen prior to mixing. Single resonance spectra indicated gases used were of stated purity.

ANALYSIS OF SPECTRA

The effect of elastic collisions on ion motion can be described as indicated in Eq. (17) by adding to the Lorentz force a term that represents the damping of the

ion velocity[21]:

$$\frac{d\mathbf{v}}{dt} = \frac{q\mathbf{E}(t)}{m} + \frac{q\mathbf{v}\times\mathbf{H}}{mc} - \xi\mathbf{v} \ . \tag{17}$$

In Eq. (17) $\mathbf{v}$ is the ion velocity, q is the charge on the ion, $\mathbf{E}(t)$ is the electric field, m is the mass of ion, H is the magnetic field, and c is the speed of light in a vacuum. If the ion experiences only elastic collisions with the neutral species, the collision frequency for momentum transfer, ξ, is given by

$$\xi = \langle \sigma_d(v_0) v_0 \rangle nM/(m+M) \ , \tag{18}$$

where n and M are the number density and mass of the neutral, and $\sigma_d(v_0)$ and v_0 are the diffusion cross section and relative velocity of the ion–neutral pair. The brackets indicate an average over the distribution of relative velocities.

With the observing radio-frequency electric field $\mathbf{E}(t)$ expressed by

$$\mathbf{E}(t) = E_1 \sin\omega t\mathbf{i} \ , \tag{19}$$

the power absorption calculated from the solution of Eq. (17) has the Lorentzian form given by

$$A(\omega_c) = \frac{I(0)\tau q^2 E_1^2}{4m} \frac{\xi}{(\omega-\omega_c)^2+\xi^2} \ , \tag{20}$$

where $\omega_c = qH/mc$ is the cyclotron frequency of the ion, $I(0)$ is the rate of ion formation at the electron beam, and τ is the time the ion spends in the resonance region of the cyclotron resonance cell. The half-width at half-height for the power absorption expression [Eq. (20)] is equal to ξ. The reduced collision frequency for momentum transfer, ξ/n, can thus be obtained directly from the slope of the variation of linewidth with pressure. Since the power absorbed at resonance is inversely proportional to ξ, the reduced collision frequency may also be obtained from the variation of the power absorption at resonance with pressure as shown by Huntress.[9] Other detailed treatments of power absorption in cyclotron resonance experiments have attempted to include the effect of reactive collisions and the finite lifetime of the ions in the apparatus.[22] Such factors are important when examining reactive ions or working in the low pressure region (10^{-5}–10^{-4} torr). We have for this reason purposefully selected ionic species for study which are nonreactive toward methane and hydrogen.

The solution of Eq. (17) involves the assumption that the collision frequency ξ is effectively independent of the velocity, v_0, over the range of velocities sampled as the ion absorbs power from the observing field. An equation of motion for the energy of the average ion, subject to the same limitations of Eq. (17), can be developed and solved with suitable approximations to give (at resonance)[21]

$$E_{\text{ion}} = 3/2kT + \frac{e^2E_1^2(m+M)}{8\xi^2m^2} \ , \tag{21}$$

where T is the temperature of the neutral species. Since ξ increases with the neutral number density [Eq. (18)], Eq. (21) indicates that the excess kinetic energy of the ion resulting from its interaction with the observing field increases with the ratio of E_1 to the pressure of the neutral. The analysis leading to Eq. (20) can thus be assumed to be valid over the range of E_1/P for which the ratio of linewidth to pressure is found to be independent of E_1/P.

The ratio of field strength to pressure is a parameter frequently used to characterize the results of dc drift tube mobility measurements. As pointed out in Appendix A, the ion cyclotron resonance experiment can be considered a dc mobility experiment in a rotating frame with a dc field equal to $E_1/2$. For this reason, the values of E_1/P reported below should be divided by 2 before comparisons are made with drift tube mobility results.

The pressure range over which experimental data can be meaningfully obtained and analyzed with Eq. (20) is limited at higher pressures by the transverse diffusion of ions which occurs as a peculiar and previously unrecognized feature of the cell geometry illustrated in Fig. 1. In addition to the observing radio frequency electric field, ions in the cell are acted upon by a constant electric field in the $-x$ direction (Fig. 1) which gives rise to the drift motion described by Eq. (1). Equation (1) is obtained from a solution of Eq. (17) for the motion in absence of collisions ($\xi = 0$). It is necessary to consider what effect collisions might have on the drift motion. Since the equation of motion which includes the effect of collisions [Eq. (17)] is linear in both ion velocity and electric field, it can be solved separately for the drift and radio frequency electric fields and the resulting solutions superimposed to give a complete description of the motion. The time averaged solution to the equation involving the drift field yields[23]

$$v_x = -\frac{\xi qE}{m(\omega_c^2+\xi^2)} \ , \tag{22}$$

$$v_y = -\frac{\omega_c qE}{m(\omega_c^2+\xi^2)} \ . \tag{23}$$

In the limit of no collisions v_x is zero and v_y yields the drift velocity expressed by Eq. (1). Collisions thus give rise to a drift velocity transverse to the usual direction of ion motion through the cell. From simple geometric considerations this motion can result in the collision of ions with the drift electrodes before the ions leave the resonance region. This condition develops when the ratio v_x/v_y is greater than half the cell height divided by the distance from the electron beam to the end of the resonance region. This occurs in our apparatus when the ratio v_x/v_y is greater than 0.0714. In order to avoid the complicating effects of this ion loss mechanism, we have confined the measurements discussed in the following section to pressures such that Eq. (24) is true:

$$v_x/v_y = \xi/\omega_c < 0.0714 \ . \tag{24}$$

RESULTS

Ions in methane

As illustrated in Fig. 2, the observed line shapes of the cyclotron resonance power absorption of CH_5^+ ions

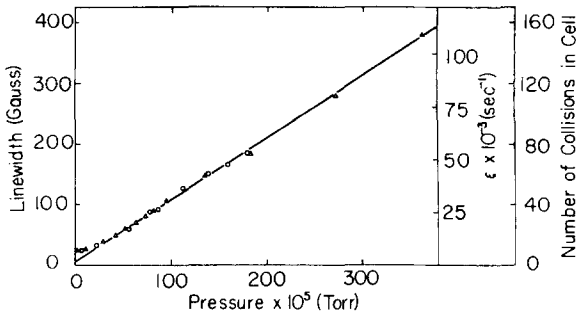

FIG. 3. Variation of CH_5^+ linewidth in gauss (full-width at half-height) with pressure. The half-width at half-height in $sec^{-1}(\xi)$ and the number of collisions suffered by the ion as it passes through the cell $[\xi\tau(m+M)/m]$ are also indicated. The circles and triangles represent data taken on two different days.

in methane fit the Lorentzian description well. The variation with pressure of the linewidth of CH_5^+ in methane is illustrated in Fig. 3. The linewidth is expressed both as the full-width at half-height in gauss and as the half-width at half-height, ξ, in sec^{-1}. The reduced collision frequency collision frequency for CH_5^+ in methane, obtained from a least squares analysis of the data above 5×10^{-4} torr in Fig. 3, is $\xi/n = 9.06 \pm 0.06 \times 10^{-10}$ cm^3 molecule^{-1} · sec^{-1} (Table I). Below 5×10^{-4} torr the linewidth approaches a low pressure limit. The limit observed is 20 ± 1 G. The observed low pressure linewidths are the result of the finite residence time of the ion in the cell and the effect of the trapping field on the ion motion. The departure of an ion from the cell has the effect of a collision in which the ion loses all of its momentum. Thus a calculation of power absorption in the absence of collisions indicates that the linewidth depends on τ, the ion residence time.[22a] As discussed elsewhere,[24] the trapping field gives rise to a shift in the resonance frequency. The shift is the same for all ions in the cell only if the spacing between the trapping electrodes is equal to the spacing between the drift electrodes. In the cell employed in our experiments the spacing between the drift electrodes is one-half that of the trapping electrodes. This results in a shift in resonance frequency dependent on the position of the ion in the trapping cell, which causes a slight broadening of the absorption line.

The data in Fig. 3 are recorded at a constant observing oscillator level of 0.0365 V cm^{-1}. This corresponds to a variation of the ratio of electric field strength to pressure from 65 to 11 V cm^{-1} · torr^{-1} over the corresponding pressure range from 5.62×10^{-4} to 3.44×10^{-3} torr. Any significant dependence of linewidth on E_1/P would cause curvature which is not observed in the data shown in Fig. 3. The linewidth is thus relatively independent of E_1/P over this range. Utilizing Eq. (21), a value of E_1/P of 65 V cm^{-1} · torr^{-1} corresponds to an estimated ion energy of 0.067 eV in excess of $\frac{3}{2}kT$ (= 0.039 eV at 300 °K).

$C_2H_5^+$, a second abundant species in methane, is produced by the following reaction:

$$CH_3^+ + CH_4 \rightarrow C_2H_5^+ + H_2 \,. \qquad (25)$$

Like CH_5^+, $C_2H_5^+$ is stable against further reaction with methane. The experimental value of ξ/n, obtained from the slope of a plot analogous to Fig. 3, is $5.39 \pm 0.12 \times 10^{-10}$ cm^3 molecule^{-1} · sec^{-1} (Table I).

Propyl and butyl cations were generated by the chemical ionization reactions[25]

$$\left.\begin{matrix} CH_5^+ \\ C_2H_5^+ \end{matrix}\right\} + C_3H_8 \rightarrow C_3H_7^+ + \left\{\begin{matrix} CH_4 + H_2 \\ C_2H_6 \end{matrix}\right. \qquad (26)$$

$$\left.\begin{matrix} CH_5^+ \\ C_2H_5^+ \end{matrix}\right\} + (CH_3)_3CH \rightarrow C_4H_9^+ + \left\{\begin{matrix} CH_4 + H_2 \\ C_2H_6 \end{matrix}\right. \qquad (27)$$

in methane containing 3% propane and isobutane, respectively. The variation with pressure of the single resonance intensities of the main ionic species in the methane–propane mixture is illustrated in Fig. 4. Above 5×10^{-4} torr, the decrease in CH_5^+ and $C_2H_5^+$ intensities with a simultaneous increase in $C_3H_7^+$ intensity indicates the occurrence of Reaction (26). The chemistry of the methane–propane mixture with $C_4H_9^+$ the predominant species at high pressure. The structure of the propyl and butyl cations generated in Reactions (26) and (27) are somewhat uncertain. In the case of propane, for instance, the species produced are probably a mixture of 2-propyl and 1-propyl cations. On subsequent collisions with propane, the 1-propyl cations are probably converted to 2-propyl cations. In the present studies, linewidths were recorded over the pressure region from 10^{-4} to 3×10^{-3} torr and most likely samples collision frequencies for several carbonium ion structures. The possibility exists that the

TABLE I. Results of collision frequency determinations.

Neutral	Ion	K_0(cm$^2V^{-1}$ · sec^{-1})[a] Measured	Polarization[c]	$\xi/n\times10^{10}$(cm^{3}mole^{-1} · sec^{-1})[b] Measured	Polarization[d]
CH_4	CH_5^+	2.32 ± 0.02	2.99	9.06 ± 0.06	7.04
	$C_2H_5^+$	2.28 ± 0.06	2.67	5.39 ± 0.12	4.62
	$C_3H_7^+$	1.99 ± 0.03	2.51	4.18 ± 0.05	3.31
	$C_4H_9^+$	1.98 ± 0.07	2.43	3.17 ± 0.09	2.59
	Na^+	3.11 ± 0.06	2.80	5.01 ± 0.09	5.57
H_2	H^+	16.2 ± 0.6	18.95	21.9 ± 0.9	18.78
	H_3^+	11.03 ± 0.14	14.19	10.78 ± 0.11	8.37
	CH_5^+	11.34 ± 0.04	11.61	1.852 ± 0.006	1.81
	H_3O^+	11.06 ± 0.19	11.54	1.703 ± 0.028	1.63
	N_2H^+	11.07 ± 0.10	11.35	1.115 ± 0.009	1.09
	$C_2H_5^+$	11.68 ± 0.21	11.35	1.056 ± 0.017	1.09
	$C_3H_7^+$	11.17 ± 0.07	11.23	0.744 ± 0.004	0.75
	Na^+	11.77 ± 0.18	11.46	1.325 ± 0.020	1.361

[a]The mobility at 273 °K and 760 torr calculated from the measured collision frequencies as indicated in the text.
[b]Determined from ion cyclotron resonance linewidth measurements. The error estimates represent standard deviations determined from a least squares analysis of linewidth vs pressure data. The accuracy of these numbers is limited to ± 2% by the pressure determination.
[c]Calculated from Eq. (9).
[d]Calculated from Eq. (38).

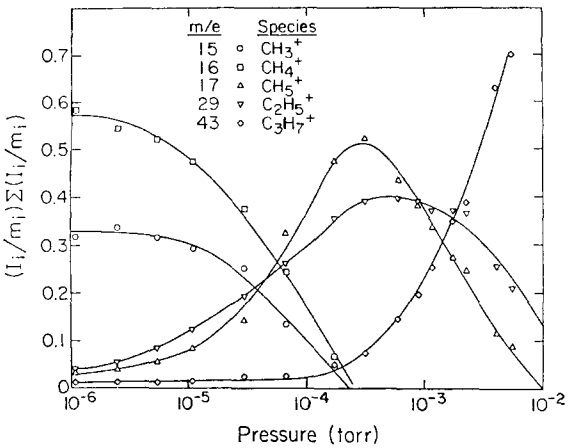

FIG. 4. The variation of relative ion abundances of ions in methane containing about 3% propane. The quantity (I_i/m_i) is the ratio of the single resonance intensity of an ion to its mass and is approximately proportional to the relative abundance of the ion (Ref. 1). Ionizing energy is 20 eV.

collision frequencies may depend on ion structure, as discussed below.

The experimental values of ξ/n for $C_3H_7^+$ and $C_4H_9^+$ are $4.18 \pm 0.05 \times 10^{-10}$ and $3.17 \pm 0.09 \times 10^{-10}$ cm^3 molecule^{-1} · sec^{-1}, respectively. The linewidth vs pressure plots in each case were linear indicating that ξ/n is independent of E_1/P. The measured values of ξ/n were corrected for the presence of the additive gases. For the purposes of these corrections, the collision frequencies of $C_3H_7^+$ and $C_4H_9^+$ with C_3H_8 and C_4H_{10} were assumed to be equal to the polarization limit discussed below. These estimates of the collision frequencies and the known partial pressures of the additives were used to estimate the contributions of the additive gases to the linewidths. The corrections were found to be very small (0.1% or 0.2%) for the partial pressures used (additives made up approximately 3% of the total pressure).

The Na^+ linewidths increased linearly with pressure, indicating ξ/n is not dependent on E_1/P. The value of ξ/n obtained for Na^+ was $5.01 \pm 0.09 \times 10^{-10}$ cm^3 molecule^{-1} · sec^{-1}.

Ions in hydrogen

The ions H^+ and H_3^+ can be directly studied in hydrogen, the latter species being generated in the reaction

$$H_2^+ + H_2 \rightarrow H_3^+ + H \ . \tag{28}$$

Other ionic species studied in hydrogen include CH_5^+, H_3O^+, N_2H^+, $C_2H_5^+$, and $C_3H_7^+$, generated in the chemical ionization reactions

$$H_3^+ + CH_4 \rightarrow CH_5^+ + H_2 \ , \tag{29}$$

$$H_3^+ + H_2O \rightarrow H_3O^+ + H_2 \ , \tag{30}$$

$$H_3^+ + N_2 \rightarrow N_2H^+ + H_2 \ , \tag{31}$$

$$H_3^+ + C_2H_6 \rightarrow C_2H_5^+ + 2H_2 \ , \tag{32}$$

$$H_3^+ + C_3H_8 \rightarrow C_3H_7^+ + 2H_2 \ . \tag{33}$$

Reactant gases were introduced as in the case of methane except that lower additive concentrations were employed, typically 0.5%. These lower concentrations were necessitated by the fact that because of its low mass, H_2 is very inefficient in comparison to the additives in momentum relaxation processes. Corrections were estimated as in the case of methane and were found to be small (1% or 2%). In each case the linewidth was found to increase linearly with pressure and thus to be independent of E_1/P below 50 V cm^{-1} · torr^{-1}. The resulting values of ξ/n are summarized in Table I. The somewhat large standard deviation of H^+ is dictated by its low abundance in the mass spectrum of hydrogen.

DISCUSSION

Comparison with mobility measurements

The mobility of an ion in a gas is the proportionality constant relating the applied field E to the observed drift velocity u of the ion in the gas,

$$u = KE \ . \tag{34}$$

The mobility is related to the collision frequency for momentum transfer ξ by[5a]

$$K = q/m\xi \ . \tag{35}$$

A derivation of Eq. (35) that relies on the fact that an ion cyclotron resonance experiment can be considered a dc mobility experiment in a rotating frame is given in Appendix A. Substituting from Eq. (18) into Eq. (35) gives

$$K = \frac{q}{n\mu\langle\sigma_d(v_0)v_0\rangle} \tag{36}$$

relating the mobility to the neutral number density and the diffusion cross section. Since the mobility is dependent on the neutral number density, the number usually reported is K^0, which is related to K by

$$K^0 = K\,\frac{P}{760}\,\frac{273}{T} \ , \tag{37}$$

where P and T are the pressure in torr and the temperature in degrees Kelvin at which K is measured. The experimental values of K^0 given in Table I were calculated from the experimental values of ξ/n in Table I using the relationships given in Eqs. (35) and (37). These numbers thus correspond to the mobility of ions in a gas at ambient temperature (298 °K) and at a density equal to that of an ideal gas at 273 °K and 760 torr. The values of ξ/n listed in Table I as polarization values are those given by Eq. (38) derived from Eqs. (8) and (35):

$$\xi/n = 2.210q\,\frac{\mu^{1/2}\alpha^{1/2}}{m} \ . \tag{38}$$

Mobilities of the systems listed in Table I that have been measured by other methods are compared with the present results in Table II. Each of the methods used to obtain the tabulated results made provision for mass identification of the charge carrying species.

The agreement between the present ion cyclotron resonance linewidth measurements and the drift tube mea-

TABLE II. Comparison of mobility measurements.

Neutral	Ion	$K_0(cm^2V^{-1}\cdot sec^{-1})$[a] This work[b]	Reference 10	Reference 12[c]	Reference 5a	Reference 9
H_2	H^+	16.2±0.6	15.7±0.6			
H_2	H_3^+	11.03±0.14	11.1±0.5	6.2±0.2	7.2	10.9±0.2
H_2	Na^+	11.77±0.18	12.2±0.6			
CH_4	CH_5^+	2.32±0.02		1.75±0.03		
CH_4	$C_2H_5^+$	2.28±0.02		1.74±0.07		

[a]The mobility at neutral density equal to that of an ideal gas at 273 °K and 760 torr.
[b]As in Table I, error estimates are an indication of precision. Accuracy is limited to ±2% by pressure determination.
[c]See text for discussion of accuracy of these measurements.

surements of McDaniels and co-workers[10] is very good. The agreement with Huntress' result[9] is also good, indicating that analysis of ion cyclotron resonance line shapes does give accurate ion neutral collision frequencies in the case where the mobility is independent of E/P. The disparity between the present results and the early ion cyclotron resonance results of Wobschall and co-workers[5] must be the result of experimental problems with the technique in its early stages of development. The problems restricting the accuracy of Wobschall's measurements may have been the lack of techniques to measure pressures less than a micron very accurately and the difficulty of characterizing the ion motion in the early soleniodal ion cyclotron resonance apparatus. The availability of the capacitance manometer for low pressure measurement, and the development of the cell design illustrated in Fig. 1, have largely alleviated these problems.

The apparatus used by Meisels and co-workers[12] was designed for chemical ionization studies and is not well suited for the measurement of accurate mobilities. The sources of error are systematic, however, and relative measurements of mobilities of various ions in the same gases should be quite reliable. The agreement between the present measurements and Meisels' measurements can thus be considered satisfactory.

Two different workers have measured the drift velocities of ions formed in discharges in methane.[26] The ions were not identified. The range of E/P values over which the measurements were made is 50–200 V cm^{-1} · $torr^{-1}$. The mobility of the charge carriers was observed to be approximately 2.5 $V^{-1}cm^2sec^{-1}$ in both cases. This agrees reasonably well with the mobilities of CH_5^+ and $C_2H_5^+$ in Table I.

Buttrill[8] reports that his measurements of linewidths of ions in hydrogen agree with our measurements but that his measurement of the CH_5^+ linewidth in methane at 300° is some 15% lower than ours, corresponding to a mobility 15% higher than ours. Buttrill suggests that the discrepancy may be the result of the fact that he made his measurements at a value of E_1/P considerably larger than the values we used. The analysis of our results in terms of mobility theory suggests that the CH_5^+ mobility may increase above the low field limit if E_1/P is several times the values we used.

Comparison with theory

In Figs. 5–8, the mobilities derived from the measured linewidths are compared with mobilities calculated from theoretical models. The solid lines labeled with γ values in Figs. 5 and 7 were calculated from the 12–6–4 potential. The solid lines labelled with a^* values in Figs. 6 and 8 were calculated from the acentric potential. The solid lines in Figs. 5 and 7 labeled "Langevin" were calculated from the Langevin potential. With the exception of H^+, the experimental points were plotted by estimating r_m from gas kinetic data and calculating the size parameters from Eqs. (13)–(16). The r_m estimate for H^+ is based on *ab initio* calculations of the H_3^+ potential surface.[27]

Except for H^+ and H_3^+, which are discussed below, the ions in hydrogen have mobilities close to K_p. This would appear to indicate that interactions other than the ion–induced dipole interaction have little effect on the mobility. The ion–neutral potential, however, must

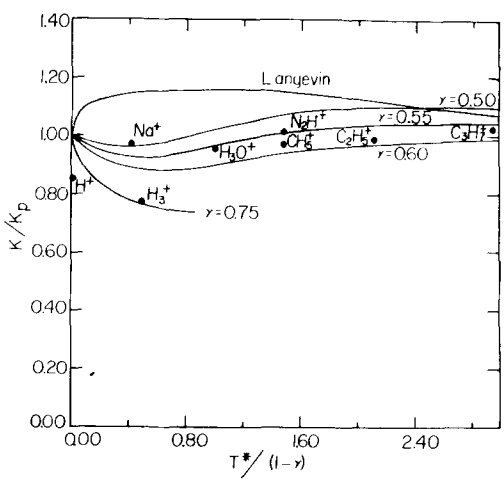

FIG. 5. The variation of the mobilities of ions in hydrogen with ion size and temperature. The quantity on the ordinate increases with ion size and temperature [Eq. (14)] and the quantity on the abscissa is the ratio of the measured K to the polarization limit K_p. Experimental points represent the results of the present study. The line called "Langevin" represents the behavior predicted by the Langevin model [Eq. (3)]. The remaining lines represent predictions from the 12–6–4 potential [Eq. (4)] with various values of the parameter γ.

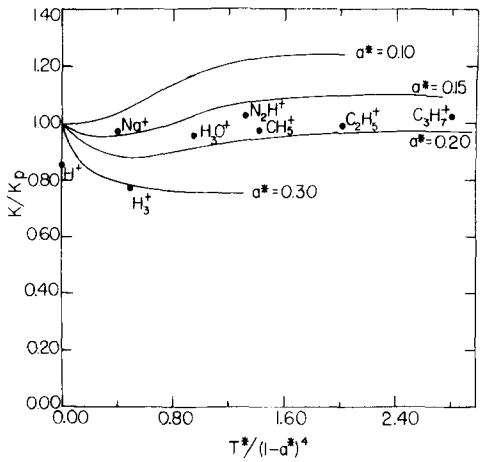

FIG. 6. The variation of the mobilities of ions in hydrogen with ion size and temperature. The quantity on the ordinate increases with ion size and temperature [Eq. (15)]. The quantity on the abscissa is the ratio of the measured K to the polarization limit K_p. Experimental points represent the results of the present study. The lines represent predictions from the acentric potential [Eq. (5)] with various values of the parameter a^*.

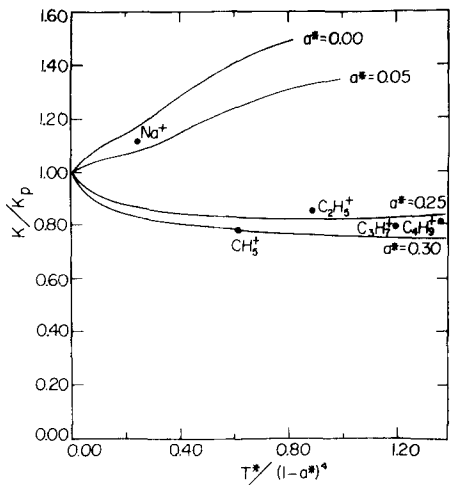

FIG. 8. The variation of the mobilities of ions in methane with ion size and temperature. The quantity on the ordinate increases with ion size and with temperature [Eq. (15)]. The quantity on the abscissa is the ratio of the measured K to the polarization limit K_p. Experimental points represent the results of the present study. The lines represent predictions from the acentric potential [Eq. (5)] with various values of the parameter a^*.

become strongly repulsive at some separation greater than zero. From an examination of Figs. 5 and 6, it is evident that only those potentials including significant medium range attractive forces are consistent with both the observed mobilities and a reasonable short range repulsion. The mobility of CH_5^+, for example, would fall on the Langevin line only if the hard sphere radius of the H_2–CH_5^+ pair were 4.3 Å compared with 3.4 Å for the Lennard-Jones radius of the H_2–CH_4 pair.[28] Similarly, a pure 12–4 potential ($\gamma = 0$ or $a^* = 0$) would account for the observed mobility only if the H_2–CH_5^+ potential became repulsive at 6.5 Å. Both experimental and theoretical results indicate that at least for

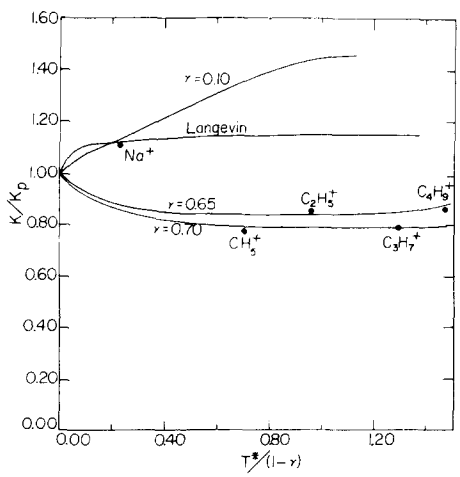

FIG. 7. The variation of the mobilities of ions in methane with ion size and temperature. The quantity on the ordinate increases with ion size and temperature [Eq. (14)] and the quantity on the abscissa is the ratio of the measured K to the polarization limit K_p. Experimental points represent the results of the present study. The line labeled "Langevin" represents the behavior predicted by the Langevin model [Eq. (3)]. The remaining lines represent predictions from the 12–6–4 potential [Eq. (4)] with various values of the parameter γ.

atomic closed shell systems the kinetic radius of a neutral–cation pair is 0.5 to 0.9 Å less than that of an isoelectronic neutral–neutral pair.[29] Thus, reasonable ion–neutral radii are generally consistent only with the potentials which include medium range attractive terms in addition to the ion–induced dipole term.

The hard sphere model accounts adequately only for the $C_3H_7^+$ mobility in H_2, which corroborates Patterson's observation that the mobilities of very large ions in gases of low polarizability are consistent with the hard sphere model.[11] It is of interest to note that N_2H^+ and $C_2H_5^+$ have measurably different mobilities even though they have the same mass. This substantiates the conclusion that the mobilities are sensitive to ion structure.

The mobilities of all the ions but Na^+ in methane are well below the polarization limit. Interactions other than the polarization interaction must be significant in the ion–molecule potentials that determine these mobilities. As indicated in Figs. 7 and 8, simply adding a repulsive interaction to the polarization potential is even less satisfactory than in the hydrogen systems. Only for very large ionic radii does the mobility calculated from the 12–4 and Langevin models fall below the polarization limit. D_{12} for the Langevin model would have to be 5.8 Å and the 12–4 potential would have to become repulsive at 9.0 Å to obtain the measured CH_5^+–CH_4 mobility. The Lennard-Jones radius for CH_4–CH_4 is 3.8 Å. Furthermore, both Langevin and 12–4 potentials give a CH_5^+–CH_4 binding energy less than 1 kcal/mole, in contradiction to results of recent experimental measurements discussed below.[30] The evidence thus indicates that medium range attractive forces are even more important in the ion–methane interactions than in the ion–hydrogen interactions.

There are several possible sources of medium range

attractive ion molecule forces. London dispersion and ion–induced dipole forces, both of which vary as r^{-6}, can be estimated from theoretical considerations by the method of H. Margenau.[31] For the $CH_5^+-H_2$ pair, for example, the estimated ratio of the coefficient of the r^{-6} term to that of the r^{-4} term is 4.0 Å^2. The ratio estimated for the $CH_5^+-CH_4$ pair is 6.5 Å^2. The values of these ratios suggested by the data, however, are 26 Å and 56 Å^2, respectively. This discrepancy between theory and experiment is best explained as indicating that forces other than London dispersion and ion–induced quadrupole forces are important in these systems. The success of the acentric potential in accounting for the observed mobilities suggests that constraints on the charge distributions of the ion and the molecule imposed by their polyatomic structures may give rise to the additional attractive forces. Valence forces similar to those involved in hydrogen bonding may also play a role since most of the ions are acidic to some extent.

It is conceivable in the $CH_5^+-CH_4$ and $H_3^+-H_2$ systems that long range symmetrical proton transfer, an efficient momentum transfer mechanism, affects the observed mobilities. The rates of proton transfer in these systems are small, however. The $H_3^+-H_2$ rate is 3×10^{-10} cm^3 molecule^{-1} · sec^{-1} [32] and the $CH_5^+-CH_4$ rate is 3×10^{-11} cm^3 molecule^{-1} · sec^{-1}.[33] Thus, proton transfer probably occurs only on intimate collisions which would involve considerable momentum transfer anyway, and it seems reasonable to assume the mobilities unaffected by proton transfer.

The mobility of the Na^+ ion in methane is unique in several ways. First, it can be accounted for by all three theories. Second, it is the only mobility significantly larger than K_p. Finally, the value of the ratio of coefficients of the r^{-6} and r^{-4} terms estimated quantum mechanically agrees well with that implied by the data. These observations provide further evidence that the polyatomic structure of the other ions is responsible for the behavior of their mobilities. It should be noted, however, that the mobility of Na^+ in H_2 can only be accounted for by the acentric and 12–6–4 potentials and, in that respect, behaves the same as the other heavy ions in H_2.

Mason and Schamp[15] point out that the E/P dependence of the mobility is related to its temperature dependence. If the mobility is approximately independent of temperature it will be approximately independent of E/P. It is evident from Figs. 5–8 that a value of γ greater than 0.50 or a value of a^* greater than 0.15 implies a mobility that does not depend strongly on temperature over the range of T^* illustrated in the figures. This range of T^* corresponds to the temperature range between ambient and 600 or 700 °K for most of the ions. Thus, only the mobility of Na^+ in methane would be expected to depend strongly on E/P. We estimate from expressions given by Mason and Schamp,[15] however, that Na^+ varies by no more than 3% over the range of E/P used in the present experiments. Thus, it is not surprising that we see no evidence of variation of any of the mobilities with E/P.

Some information on several ion–hydrogen and ion–methane interaction potentials is available from scattering experiments, equilibrium constant measurements, and *ab initio* calculations. Recent *ab initio* calculations suggest that the best parameters for an angle averaged H^+-H_2 potential would be $r_m = 0.9$ Å and $\epsilon = 3.8$ eV.[27] When these values are substituted into Eqs. (14) and (15), however, negative values of γ and a^* result. Thus, both 12–6–4 and acentric potentials seem to be inadequate models of the H^+-H_2 system. This is not too surprising, since these potentials are intended to model electrostatic or weak bonding interactions and H_3^+ is a very stable chemically bound species.

The $H_3^+-H_2$, $CH_5^+-CH_4$, and $C_2H_5^+-CH_4$ bond enthalpies are known from mass spectrometric studies of the appropriate dissociation equilibria.[30,34] Potential well depths determined from the bond enthalpies are given in Table III. The remaining parameters for the 12–6–4

TABLE III. Parameters for intermolecular potentials.

	12–6–4 Potential[a]				Acentric Potential[b]			
Interacting pair	$\epsilon\times10^{13}$[c] (ergs)	$r_m\times10^8$ (cm)	$\sigma_0\times10^8$ (cm)	γ	$\epsilon\times10^{13}$[c] (ergs)	$r_m\times10^8$ (cm)	$\sigma_0\times10^8$[d] (cm)	$a\times10^8$ (cm)
$CH_5^+-CH_4$	2.46	4.12	3.65	0.72	2.46	4.25	3.86	1.25
$C_2H_5^+-CH_4$	1.24	4.60	4.04	0.64	1.24	4.62	4.16	1.06
$H_3^+-H_2$	6.32	2.58	2.27	0.78	6.32	2.72	2.45	0.95
CH_4-CH_4[e]	0.19	4.31	3.84	1	0.24	4.19	3.72	0.21
$C_2H_6-CH_4$[e]	0.26	4.64	4.13	1				
H_2-H_2[e]								

[a]Equation (4).
[b]Equation (5).
[c]Binding energies for ion–molecule pairs are from Refs. 30 and 34.
[d]σ_0 is the value of r at which $V(r)$ goes to zero.
[e]Except for the parameters for CH_4-CH_4 acentric potential which are from F. Danon and K. S. Pitzer, J. Chem. Phys. **36**, 425 (1962); the parameters for the neutral–neutral potentials are from J. O. Hirschfelder, C. F. Curtiss, and R. B. Bird, *Molecular Theory of Gases and Liquids* (Wiley, New York, 1954). The ethane-methane parameters are the averages of the CH_4-CH_4, and $C_2H_6-C_2H_6$ parameters.

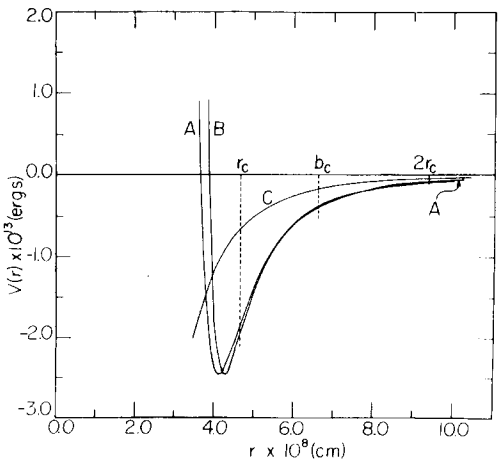

FIG. 9. The 12–6–4 (A), acentric (B), and polarization (C) potentials for the CH_5^+–CH_4 system. The 12–6–4 and acentric potential parameters were determined from the present mobility measurements and a binding energy determined from equilibrium studies as described in the text. The polarization potential was calculated from Eq. (3). The orbiting impact parameter b_c and corresponding radius r_c for the polarization potential were calculated using Eqs. (39) and (40) and assuming $1/2\mu v_0^2 = 3/2kT$ and $T = 300\,^\circ$K.

and acentric potentials can be determined from the well depths and the measured mobilities and are also given in Table III. Although the 12–6–4 and acentric potentials have two disposable parameters besides the neutral polarizability, there is only one combination of the two parameters consistent with the experimental well depth and mobility. The resulting ion–neutral radii are all slightly less than comparable neutral–neutral radii. This suggests the 12–6–4 and acentric potentials represent the true potential surfaces much better than the simpler Langevin or 12–4 potentials. Calculations on H_5^+[35] suggest an H_2–H_3^+ separation of 2.1 Å in the most stable configuration. Considering that the mobility averages the effects of many different collisional configurations, the agreement with r_m in Table III (2.6–2.7 Å) is reasonably good. This agreement is certainly much better than that provided by the 12–4 and Langevin potentials, which give the observed H_3^+–H_2 mobility only if $r_m = 7.7$ Å and $D_{12} = 5.1$ Å. In addition, the 12–4 and Langevin potentials require a binding energy less than 1 kcal/mole.

The acentric and 12–6–4 representations of each of these interactions are very similar. This is illustrated for CH_5^+–CH_4 in Fig. 9. The similarity of the two curves suggests that the actual potential surface must share their essential features. One interesting feature of the two curves is that they differ from the polarization potential at long range. It is commonly assumed that the latter interaction is completely dominant at long range. The cross section for classical orbiting,

$$\sigma_p = 2\pi q(\alpha/\mu v_0^2)^{1/2}, \tag{39}$$

calculated from the polarization potential is, in fact, frequently considered a theoretical upper limit for ion–molecule reaction cross sections.[36] Indicated on Fig. 9 are the maximum impact parameter b_c and corresponding orbital radius r_c for classical orbiting calculated from the polarization potential with $\mu v_0^2 = 3kT$ and $T = 300\,^\circ$K. Only if the actual potential be nearly equal to the polarization potential at all $r > r_c$ is σ_p an upper limit for reaction cross sections. This evidently is not the case in the present instance, and a more satisfactory limit is the orbiting cross section obtained from the 12–6–4 or acentric potentials. Collision frequencies for orbiting obtained from the 12–6–4 and acentric potentials are compared with those for the polarization potential

$$k_p = 2\pi e\left(\frac{\mu}{\alpha}\right)^{1/2} \tag{40}$$

in Table IV. The orbiting collision frequency k is related to the orbiting cross section $\sigma(v_0)$ by

$$k = \sigma(v_0)v_0 \tag{41}$$

and is tabulated rather than the cross section since it is directly comparable with reaction rate constants. The large values of k/k_p obtained clearly reflect the difference between the polarization interaction and the potential implied by the mobility. Orbiting collisions evidently occur as much as 50% more frequently than the polarization potential predicts. This result is relatively insensitive to the accuracy of the mobility and bond enthalpy measurements. An error of 20% in the mobility and 50% in the bond enthalpy still implies a k/k_p for CH_5^+–CH_4 of 1.25. It is interesting to note that k/k_p for Na^+–CH_4 from the measured mobility and an estimated Na^+ radius is 1.00. These results suggest that the upper limit for reaction or the orbiting collision frequency for an ion–neutral pair may be sensitive to the structure of both the ion and neutral even for an isotropic molecule like methane.

SUMMARY AND CONCLUSIONS

Mobilities derived from ion cyclotron resonance linewidths have been found to be in very good agreement with drift tube measurements. This provides experimental substantiation for the analysis of the cyclotron resonance phenomenon relating mobilities and linewidths. The perturbation of the ion velocity distribution by the observing field is apparently small enough to obtain low field mobilities from linewidths in the systems studied where Lorentzian line shapes are observed.

Mobilities of polyatomic ions in methane and hydrogen are consistent with either a 12–6–4 or an acentric ion–molecule interaction potential. The observed mobilities

TABLE IV. Orbiting collision frequencies for 12–6–4 and acentric potentials.

	$k/2\pi e(\alpha/\mu)^{1/2}$		
	Polarization	12–6–4	Acentric
CH_5^+–CH_4	1.00	1.53	1.54
$C_2H_5^+$–CH_4	1.00	1.39	1.40
$H_3^+ + H_2$	1.00	1.43	1.43

of polyatomic ions can generally be obtained from the Langevin potential or a 12–4 potential only by assuming unreasonably large kinetic radii. In the cases of CH_5^+–CH_4, $C_2H_5^+$–CH_4, and H_3^+–H_2, the ion–neutral binding energies have been measured. These binding energies combined with the measured mobilities and neutral polarizabilities determine the three parameter potentials and overdetermine the two parameter potentials. In these cases the two parameter potentials (12–4 and Langevin) give radii that are too large and binding energies that are much too small. The three parameter potentials (12–6–4 and acentric) give quite reasonable radii and are in good agreement with each other. Orbiting cross sections calculated from the three parameter potentials for CH_5^+–CH_4 and $C_2H_5^+$–CH_4 are 50% larger than the polarization cross section. The mobility of H^+ in H_2 appears to be inconsistent with all of the interaction potentials considered. The mobility of Na^+ in CH_4 is consistent with all interaction potentials considered. The over-all conclusion suggested by comparison of measured and calculated mobilities is that the long range part of the ion–neutral potential is sensitive to ion structure. While the polarization interaction may be dominant for atomic ion–neutral pairs such as Na^+–CH_4, other interactions may be important for polyatomic ion–neutral pairs such as CH_5^+–CH_4 and $C_2H_5^+$–CH_4 and H_3^+–H_2.

ACKNOWLEDGMENTS

This research was supported in part by Atomic Energy Commission Grant No. AT(04-3)767-8. D. P. Ridge wishes to acknowledge the donors of the Petroleum Research Foundation administered by the American Chemical Society and University of Delaware Research Foundation for partial support of this research.

APPENDIX A: THE RELATIONSHIP BETWEEN CYCLOTRON RESONANCE AND ION MOBILITY EXPERIMENTS

The velocity of an ion responding to the influence of a constant electric field of strength E is given by

$$v = KE \ , \tag{A1}$$

where K is defined as the ion mobility. In a cyclotron resonance experiment, the ion is subjected to a linearly polarized radio frequency electric field given by $E_1 \sin\omega t\,\mathbf{i}$, which can be broken down into the two circularly polarized counter-rotating components given by

$$E^+(t) = \tfrac{1}{2}E_1 \sin\omega t\,\mathbf{i} + \tfrac{1}{2}E_1 \cos\omega t\,\mathbf{j} \ , \tag{A2}$$

$$E^-(t) = \tfrac{1}{2}E_1 \sin\omega t\,\mathbf{i} - \tfrac{1}{2}E_1 \cos\omega t\,\mathbf{j} \ . \tag{A3}$$

We can transform the ion velocity into a coordinate system rotating with the electric field by writing

$$v_x = u \sin\omega t + w \cos\omega t \ , \tag{A4}$$

$$v_y = u \cos\omega t - w \sin\omega t \ . \tag{A5}$$

The steady state component of velocity, u, rotates in phase with the electric field $E^+(t)$, and at resonance is given by[21]

$$u = qE_1/2m\xi \ . \tag{A6}$$

As in the case of Eqs. (20) and (21), derivation of Eq. (A6) involves the assumption that the collision frequency is effectively independent of velocity over the range of velocities sampled as the ion absorbs power from the observing field. A comparison of Eqs. (A1) and (A6) gives

$$K = q/m\xi \ , \tag{A7}$$

with the factor of $\frac{1}{2}$ in Eq. (A6) accounting for the fact that only one circularly polarized component of the linearly polarized field is felt by the ion at resonance. Ion mobilities can thus be calculated directly from experimentally measured cyclotron resonance linewidths.

*NDEA Predoctoral Fellow 1971–1972.
†Present address.
‡Dreyfus Teacher Scholar 1971–1975.

[1]S. E. Buttrill, Jr., J. Chem. Phys. 50, 4125 (1969).
[2]M. T. Bowers, D. D. Elleman, and J. L. Beauchamp, J. Chem. Phys. 72, 3599 (1968).
[3]J. L. Beauchamp and S. E. Buttrill, Jr., J. Chem. Phys. 48, 1783 (1968).
[4]J. H. Futrell and T. O. Tiernan, "Ion Molecule Reactions," in *Fundamental Processes in Radiation Chemistry*, edited by P. Ausloos (Wiley Interscience, New York, 1968), Chap. 4.
[5](a) D. Wobschall, R. A. Fluegge, and J. R. Graham, Jr., J. Chem. Phys. 47, 4091 (1967); (b) D. Wobschall, Rev. Sci. Instrum. 36, 466 (1965); (c) D. Wobschall, J. Graham, Jr., and D. Malone, Phys. Rev. 131, 1565 (1963).
[6]A preliminary account of the present work appears in J. L. Beauchamp, Adv. Phys. Chem. 21, 528 (1971).
[7]P. P. Dymerski and R. C. Dunbar, J. Chem. Phys. 57, 4049 (1972).
[8]S. E. Buttrill, Jr., J. Chem. Phys. 58, 656 (1973).
[9]W. T. Huntress, J. Chem. Phys. 55, 2146 (1971).
[10]T. M. Miller, J. T. Moseley, D. W. Martin, and E. W. McDaniel, Phys. Rev. 173, 115 (1968).
[11]P. L. Patterson, J. Chem. Phys. 56, 3943 (1972).
[12]G. Sroka, C. Chang and G. C. Meisels, J. Am. Chem. Soc. 95, 1052 (1972).
[13]P. Langevin, Ann. Chim. Phys. Ser. 8, 5, 245 (1905). Translated in E. W. McDaniel, *Collision Phenomena in Ionized Gases* (Wiley, New York, 1964), Appendix II.
[14]E. A. Mason and H. W. Schamp, Jr., Ann. Phys. 4, 233 (1958).
[15]E. A. Mason, H. O'Hara, and F. J. Smith, J. Phys. B 5, 169 (1972).
[16]E. W. McDaniel, *"Collision Phenomena in Ionized Gases,"* (Wiley, New York, 1962).
[17]J. M. S. Henis and W. Frasure, Rev. Sci. Instrum. 39, 772 (1968).
[18]E. W. Rothe, J. Vacuum Sci. Technol. 1, 66 (1964).
[19]S. Dushman, *Scientific Foundations of Vacuum Technique* (Wiley, New York, 1962).
[20]J. P. Blewett and Ernest J. Jones, Phys. Rev. 50, 464 (1936).
[21]J. L. Beauchamp, J. Chem. Phys. 46, 1231 (1967).
[22](a) M. B. Comisarow, J. Chem. Phys. 55, 205 (1971); (b) A. G. Marshall, J. Chem. Phys. 55, 1343 (1971); (c) A. G. Marshall and S. E. Buttrill, Jr., J. Chem. Phys. 52, 2752 (1970); (d) See Ref. 1.
[23]J. L. Beauchamp, Ph.D. thesis, Harvard University, 1967.
[24]J. L. Beauchamp and J. T. Armstrong, Rev. Sci. Instrum. 40, 123 (1969).
[25]F. H. Field, Acc. Chem. Res. 1, 42 (1968).
[26](a) K. J. Schmidt, Z. Phys. 139, 251 (1954); (b) H. Schlumbohm, Z. Phys. 182, 317 (1965).
[27](a) I. G. Csizmadia, R. E. Kari, J. C. Polanyi, A. C.

Roach, and M. A. Robb, J. Chem. Phys. **52**, 6205 (1970); (b) H. Conroy, J. Chem. Phys. **51**, 3979 (1969).
[28]J. O. Hirschfelder, D. F. Curtiss, and R. B. Bird, *Molecular Theory of Gases and Liquids* (Wiley, London, 1954), pp. 1110–1111.
[29]Y. S. Kim and R. G. Gordon, J. Chem. Phys. **61**, 1 (1974).
[30](a) U. A. Arifov, S. L. Pozharov, I. G. Chernov, and Z. A. Mukhamediev, High Energy Chem. **5**, 69 (1971); (b) S. L. Bennet and F. H. Field, J. Am. Chem. Soc. **94**, 8669 (1972); (c) K. Hiraoka and P. Kebarle, J. Chem. Phys. **62**, 2267 (1975).
[31]H. Margenau, Philos. Sci. **8**, 603 (1941) and references therein.
[32]T. Terao and R. A. Beck, J. Phys. Chem. **73**, 3884 (1969). This rate has also been measured by T. B. McMahon and P. Miasek in this laboratory (Cal. Tech.) and found to be $\sim 3 \times 10^{-10}$ cm^3 molecule$^{-1}\cdot$ sec^{-1}.
[33]R. H. Lawrence, Jr. and R. F. Firestone, Adv. Chem. Ser. **58** (1966). This rate has also been measured in this laboratory (Cal. Tech.) by T. B. McMahon and P. Miasek and found to be about 3.5×10^{-11} cm^3 molecule$^{-1}\cdot$ sec^{-1}.
[34]F. H. Field and D. P. Beggs, J. Am. Chem. Soc. **93**, 1585 (1971).
[35](a) R. D. Poshusta, J. A. Haugen, and D. F. Zetik, J. Chem. Phys. **51**, 3343 (1969); (b) W. I. Salmon and R. D. Posthusta, J. Chem. Phys. **59**, 4867 (1973).
[36]For examples, see (a) G. Gioumousis and D. P. Stevenson, J. Chem. Phys. **29**, 294 (1958); (b) S. K. Gupta, E. G. Jones, A. G. Harrison, and J. J. Myher, Can. J. Chem. **45**, 31 (1967); (c) F. C. Fehsenfeld, A. L. Schmeltekupf, and E. E. Furgeson, J. Chem. Phys. **46**, 2802 (1967); (d) M. T. Bowers and D. D. Elleman, Chem. Phys. Lett. **16**, 486 (1972); (e) L. Hellner and W. L. Sieck, J. Res. Natl. Bur. Stand. Sect. A **75**, 487 (1971).